

Chapter 1

Climate Variability and Changes in Precipitation Extremes and Characteristics

Ramesh S. V. Teegavarapu

Abstract Climate variability and change are expected to bring several changes to hydrologic cycles and regimes in different parts of the world. Natural climate variability based on large-scale, global inter-year, quasi-decadal and decadal, and multidecadal-coupled oceanic–atmospheric oscillations (e.g., El Niño Southern Oscillation (ENSO), Atlantic Multidecadal Oscillation (AMO) and Pacific Decadal Oscillation (PDO), Madden–Julian Oscillation (MJO), Indian Ocean Dipole (IOD)) contribute to regional variations in extremes and characteristics of essential climatic variables (e.g., temperature, precipitation, etc.) in different parts of the globe. These oscillations defined based on climate anomalies that are related to each other at large distances (referred to as *teleconnections*) are known to impact regional and global climate. Linkages of these teleconnections to the variability in regional precipitation patterns have been well documented in several research studies. This chapter focuses on evaluation of climate variability influences on precipitation extremes and characteristics. Several indices and metrics are discussed for such evaluation, and a few results from case studies are presented.

Keywords Climate variability • Precipitation extremes and characteristics • Coupled oceanic and atmospheric oscillations • Hydrologic design

1.1 Climate Variability: Introduction and Background

Our terrestrial environment continues to transform under the natural cyclic variations of climate and evolve due to changing climate mainly influenced by human activities. Climate variability generally denotes deviations in climatological statistics over a given period, and these deviations are usually referred to as anomalies. Variability can be associated with natural internal processes within a climate system or anthropogenic influences referred to as external forcings. Climate change on the other hand refers to a significant variation in state of the climate over an extended

R.S.V. Teegavarapu (✉)
Department of Civil, Environmental and Geomatics Engineering,
Florida Atlantic University, Boca Raton, FL, USA
e-mail: rteegava@fau.edu

period of time again linked to both internal and external anthropogenic influences. Essential climatic variables (ECVs) that have been observed, reconstructed, and projected in future by climate change models tell different stories of our changing planet's climate. Understanding these changes from the past based on limited observations and adapting to future changes based on uncertain projections of future climate derived from climate models (Teegavarapu 2010) are two main challenges faced by water management agencies. Separating clean signal of natural cyclical changes of climate from noise of human-induced changes is a difficult task we need to understand and undertake.

1.2 Coupled Oceanic–Atmospheric Oscillations

Natural climate variability on multiple timescales (ranging from inter-annual, multidecadal, and longer geologic timescales) is a major obstacle to the reliable characterization of global climate changes resulting from human activities (Ghil 2002; Gurdak, et al. 2009). Quantifying the human fingerprint on climate change and predicting future changes are two of the greatest challenges facing all scientists who are involved in understanding variability of hydrologic cycles in different regions around the world. Detection and attribution which deal with identification of trends in essential climatic variables (ECVs) and address the causes, respectively, generally lead the current climate change and impact studies. Climate change is expected to bring several changes to hydrologic cycles and regimes in different parts of the world. In addition to uncertain sea level rise rates and future changes in temperature and precipitation patterns, human-induced climate change masks the natural climate variability. This is primarily because they are dependent on large-scale, global decadal oscillation weather systems. Some of these are limited to large multidecadal sea surface temperature (SST) anomalies which have significant impacts on regional and global climate.

1.3 Inter-year, Decadal, and Multidecadal Oscillations

The following sections provide brief descriptions of inter-year, decadal, and multi-decadal oscillations.

1.3.1 El Niño Southern Oscillation (ENSO)

The ENSO is a slow oscillation in which the atmosphere and ocean in the tropical Pacific region interact to produce a slow, irregular variation between two phases: the warm and cool phase of ocean temperatures. ENSO is a major source of inter-annual climatic variability in many regions of the world. One of the indices used for

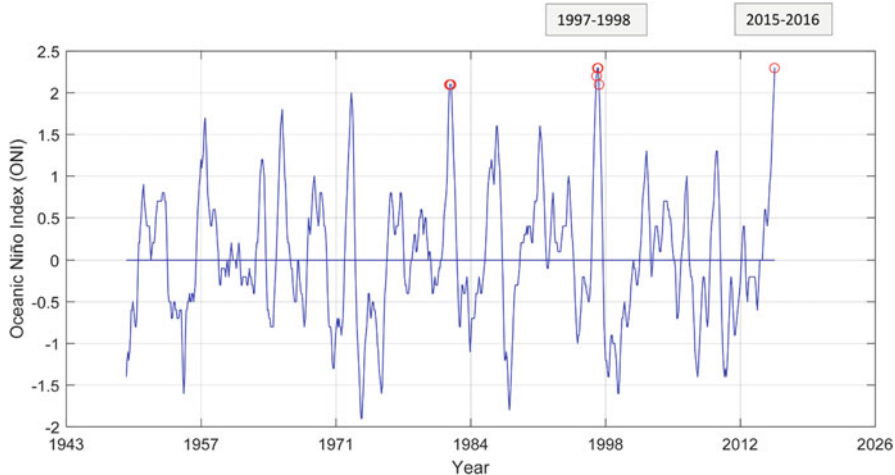


Fig. 1.1 Variation of ONI used for the determination of ENSO phases

defining two phases of ENSO is Oceanic Niño Index (ONI). The index is calculated based on observed sea surface temperature in the region that spans a swath from 5°N to 5°S latitude and 120°W to 170°W longitude. Figure 1.1 shows the ONI values and especially values above 2 indicating strong El Niño years. These variations are more commonly known as El Niño (the warm phase) and La Niña (the cool phase). Even though ENSO is centered in the tropics, the changes associated with El Niño and La Niña events affect climate around the world. ENSO events tend to form between April and June and typically reach full strength in December. ENSO is by far the most studied teleconnection and probably most publicized due to strong El Niño events of 1982–1983 and 1997–1998 which lead to the highest damages to agricultural and other sectors. ENSO is considered as the single largest cause of extremes in precipitation (as well as the cause of inter-annual variability) accounting for 15–20% of the global variance of precipitation (Dai et al. 1997). The contribution is higher than 20% in ENSO regions. These conclusions were based on monthly gridded datasets from 1900 to 1988. Studies performed by Goly and Teegavarapu (2012) indicated that El Niño is responsible for higher precipitation totals compared to La Niña in the months of December to February in Florida, USA. The conclusions were based on gridded precipitation datasets and also historical precipitation data from several rain gauges.

1.3.2 Atlantic Multidecadal Oscillation (AMO)

The Atlantic Multidecadal Oscillation (AMO) is a naturally occurring oceanic–atmospheric phenomenon on the North Atlantic Ocean that manifests in variability of SST. The AMO index is calculated using SST anomalies calculated in the region

between the latitude of 75.0°N and 0.0°S and between the longitudes of 10.0°E and 75.0°W. Temperature variations have been instrumentally observed for over 150 years, but considering paleoclimatic evidence, such as ice cores and tree rings, it can be concluded that AMO has been present for the last millennium. To better understand this naturally occurring oscillation, and its effect on extreme events, it is helpful to study past phases. SST is an indicator of a specific phase. During the warm phase, elevated SST is generally observed, while the cold phase experiences lower SST. Since instrumental temperature records are available only from 1880, the existence of two phases of AMO, dating back to the nineteenth century or earlier, can be confirmed only possible using sediment core or tree ring data. United States Geological Survey (USGS) 2011 used data from sediment core from the Gulf of Mexico and coral core from Puerto Rico and found that these two sources showed a similar variability and correlated with the instrumental temperature data of the twentieth century, concluding that SST oscillations have existed at least since the 1800s. AMO has two phases, warm and cool, with each phase lasting about 20–40 years, yielding in an approximate of 70 years long cycle. Between the extreme values of the cool and warm phases, an SST difference of 1 °F can be observed. The effects of AMO can either obscure or exaggerate the global warming due to anthropogenic sources, depending on the current phase. AMO is known to have impacts on temperature, rainfall, hurricanes, drought, or floods. There are several different studies and agencies that determine warm and cool phases for the AMO, some of which determine the intervals with gaps between them, such as Enfield et al. (2001), which lists the cool periods to be 1905–1925 and 1970–1990 and the warm periods to be 1930–1960 and 1995–2010. Some studies (e.g., Koch-Rose et al. 2011; Teegaravapu et al. 2013) have used different intervals for AMO, without leaving any gaps between them. The intervals are consecutive and include every year from 1985 to 2010. Since the phases of AMO can last up to 20 to 30 years, it is possible to make a clear distinction about the effects when studying historical data of precipitation extremes. A study published by USGS (2011) looked at the frequency of hurricane occurrences, under the different phases of AMO. Using historical data provided by the National Oceanic and Atmospheric Administration (NOAA), the number of category 4 and 5 hurricanes was counted. It was concluded that during the 26 years long negative phase, eight hurricanes made landfall, while the positive phase lasting only 13 years experienced 14 hurricane landfalls.

1.3.3 Pacific Decadal Oscillation (PDO)

The Pacific Decadal Oscillation (PDO) is an inter-decadal climate variability phenomenon characterized by changes in sea surface temperature, sea level pressure, and wind patterns. The warm and cold phases are defined by positive and negative values of PDO index, respectively. The oscillation was discovered in 1997 by Steven Hare who has conducted a study on salmon fisheries in the Pacific Northwest. PDO

is characterized by the sea surface temperature and sea level pressure change that occurs over the North Pacific Ocean (Mantua et al. 1997; Mantua and Hare 2002). Tree ring analysis suggests that this phenomenon has existed and reoccurring with 50–70 years intervals (Mantua et al. 1997). To determine the driving forces of the PDO, statistical analysis was applied on the SST, the sea level pressure (SLP), and the wind stress across the North Pacific Ocean (Schneider and Cornuelle 2005). This was done to study the temporal and spatial effects of this climate variability. The climate variations related to PDO have significant effects across the North Pacific, as well as the Americas with influences on the water resources, fisheries, and other natural habitats.

1.3.4 North Atlantic Oscillation (NAO)

The North Atlantic Oscillation (NAO) (Wallace and Gutzler 1980) is characterized by low pressure occurring over Iceland and high pressure over the Azores, which is centrally located between Portugal and North America. NAO is in the positive phase when the Icelandic low pressure and the Azores subtropical high pressure are strongly dominant. During this phase the Atlantic experiences stronger westerly winds, which bring storms in higher frequency to Europe. When NAO is in the positive (warm) phase, the east coast of North America has a milder winter with above-average temperatures and more precipitation. During the positive phase, the crossing storms are stronger and more frequent, in a northern direction. Winter conditions are warm and wet across Europe, while Canada and Greenland experience cold and dry conditions. Negative phase will occur when the pressure areas, the Icelandic low and the Azores high, are not as dominant. In this phase, the westerly winds are weaker, allowing the cold Arctic air to enter the USA and reach southern areas. There are fewer storms over the Atlantic, and the east coast of North America has a colder winter and precipitation in the form of snow. Snowstorms with subfreezing conditions occur in higher frequency over the USA. Characteristics of the negative NOA index include colder temperatures over northern Europe, while the Mediterranean experiences more moisture and milder winters. Fewer and weaker storms are crossing over the Atlantic in the west to east direction. The winter along the East Coast of the USA has more cold air outbreaks, as well as snowy weather conditions.

1.3.5 Other Major Oscillations

A number of other high- and low-frequency oscillations influence hydroclimatic variables in different regions of the world. These oscillations include Arctic Oscillation (AO), Madden–Julian Oscillation (MJO), Pacific North American (PNA)

pattern, and Indian Ocean Dipole (IOD). The IOD, referred to as the Indian Niño, is an irregular oscillation of sea surface temperatures with cool and warm phases. Exhaustive discussion about these oscillations is available elsewhere (Cronin 2009; Teegavarapu 2013; Rosenzweig and Hillel 2008).

1.4 Regional and Global Influences of Oscillations

Regional and global influences of oscillations on ECVs are documented by several studies (Cronin 2009; Teegavarapu 2013). AMO, ENSO, PDO, and NAO have influences on precipitation and temperature characteristics of the USA. The effects of PDO can be felt during winter and spring, between November and March across the USA. When PDO is in a warm phase, higher temperatures are observed across the Northwestern USA, while southeast America experiences cool temperatures. PDO is dependent upon the ENSO, because it showed more decadal variability in response to ENSO (Newman et al. 2003). The results of this study also showed that the oscillation has a strongest effect on SST across the northern part of the Pacific during winter and spring. Previously it was believed that the PDO has greater effect on the same geographical area during summer (Zhang et al. 1996). Zhang studied the inter-annual variability of SST and SLP and the Southern Oscillation Index time series. Based upon historical data, a change in the temporal variability was observed and analyzed with several techniques. This variation showed a trend that was inter-annual and consistent with an ENSO-like oscillation. In addition, a linearly independent decadal variability was also observed. This inter-decadal variability has similar properties like the ENSO, except it shows effects over the North Pacific and not confined to the equatorial area. A shift was observed in the data, around 1977, which is consistent with the phase change of PDO from cool to warm. Hurrell and Van Loon in their research paper published in 1995 studied the changes in distribution of precipitation and surface temperature over the Northern Hemisphere, more specifically the North Atlantic. These changes can be correlated with the current phase of NAO. Data about the oscillation is available for the past 150 years. When analyzing the data and the changes occurring, it was established that NAO has been in the positive phase since the 1980s. It was concluded that the precipitation anomalies of the same period can be correlated with the warm NAO phase. Anomalies include changes in temperature and precipitation. Wintertime warming over Europe and wintertime cooling of the northwest Atlantic have been recorded. Northern Europe has experienced winters wetter than usual, while winters are dryer in southern Europe. It was also concluded that as a result of the current positive phase of NAO, the storm tracks over the Atlantic have experienced a northward shift (Hurrell and Van Loon 1995). Teleconnections can be analyzed using several different parameters. Wallace and Gutzler (1980) used sea level pressure and geopotential height to find evidence of oscillation patterns of at least

a month, on the Northern Hemisphere. Correlation statistics were used to find the strongest teleconnections. After the analysis, it was concluded that the NAO and the Pacific/North Oscillation have strong presence. Also, there is a correlation between the Atlantic Jet Stream and the NAO (Wallace and Gutzler 1980). The IOD is known to have an opposing effect or neutralizing effect on the influences of El Niño on the Indian subcontinent that reduces monsoon precipitation amounts. El Niño is linked with wetter conditions in the southeastern USA, a few regions in South America and Northern Africa during the months of December–February. Also, dry conditions are known to exist in several regions of Asia including India and wet conditions in the Northwestern USA and southwestern part of South America during the months of June–August. La Niña is associated with wet conditions in few regions of the USA and drier conditions in the southeastern USA during the months of December–February. Parts of India and Asia experience wet conditions during June–August months associated with La Niña. AMO influences on precipitation with increases in extremes during warm phase in several regions of the southeastern USA are documented by Teegaravapu et al. (2013) and Goly and Teegaravapu (2014). Increased hurricane landfalls were also noted during warm phase of AMO. The temporal windows associated with cool and warm phases of ENSO and AMO are provided in Table 1.1. Similarly, the temporal windows associated with cool and warm phases of PDO and NAO are provided in Table 1.2. In many regions limited information about temporal variations in influences of oscillations are available, and spatial extent is not clearly defined.

Table 1.1 Years identified as cool and warm episodes for AMO and ENSO (1950–2010)

	AMO	ENSO ^a
Cool (La Niña)	1970–1994	1950, 1954, 1955, 1964, 1967, 1970, 1971, 1973, 1974, 1975, 1983, 1984, 1988, 1995, 1998, 1999, 2000, 2005, 2007, 2008
Warm (El Niño)	1950–1969, 1995–2010	1951, 1953, 1957, 1958, 1963, 1965, 1968, 1969, 1972, 1976, 1977, 1982, 1986, 1987, 1991, 1994, 1997, 2002, 2004, 2006, 2009
Neutral	–	1952, 1956, 1959, 1960, 1961, 1962, 1966, 1978, 1979, 1980, 1981, 1985, 1989, 1990, 1992, 1993, 1996, 2001, 2003

Source: Goly and Teegaravapu (2014), adopted with permission

^aDenotes for the current year–subsequent year, for example, 1950–1951 is represented by 1950.

Table 1.2 Years identified as cool and warm episodes for AMO and ENSO (1900–2010)

	PDO	NAO
Cool	1900–1925	1952–1972, 1977–1980
	1946–1976	
	2000–2010	
Warm	1926–1945	1950–1951, 1973–1976, 1981–2001
	1977–1999	

Source: Pierce (2013)

1.5 Evaluation of Changes in Precipitation Extremes and Characteristics

Evaluation of precipitation characteristics and extremes will involve a number of steps ranging from data collection to development of inferences about the influences of climate variability using statistical tests. The following steps are recommended for analysis of precipitation data:

- Collect and evaluate the precipitation data for different temporal and spatial scales.
- Assess missing data lengths, nonhomogeneity issues, and erroneous data.
- Fill missing data using appropriate spatial or temporal interpolation methods using available data from single- or multisensor precipitation estimates.
- Check the homogeneity of data after any infilling and note change points (if any) in the time series.
- Apply corrections to estimates (i.e., infilled data) and reevaluate the homogeneity of the time series.
- Identify temporal windows for climate variability analysis.
- Identify a list of indices that can characterize the changes in the variables (or time series of variables).
- Identify and select statistical methods for analysis of these indices: examples of these include statistical inference tests (parametric and nonparametric).
- Identify, select, and execute parametric and nonparametric trend tests if trend evaluation is required.
- Report statistically significant results from inference and trend analysis tests.
- Assess the spatial and temporal influences of climate variability on precipitation.
- Understand and document potential implications associated with the influences (noted in the previous step) of climate variability on hydrologic design, water resources management.

Spatial and temporal changes and trends in precipitation extremes and characteristics due to climate variability can be evaluated using a number of indices. These indices reflect different characteristics of precipitation time series, and they include (1) inter- and intra-annual variations, (2) seasonality, (3) spatial and temporal variability of extremes, (4) nature of extremes (based on events related to the type of storm: convective, frontal), (5) transition states as defined by rain or no-rain dichotomous events, (6) temporal persistence as defined by serial autocorrelation, (7) intra-event temporal distribution of precipitation, (8) antecedent moisture conditions (AMC) preceding extreme events, (9) temporal occurrences of extremes, (10) number of extremes over a specific threshold, (11) inter-event time definition (IETD) (based events), and (12) individual and coupled influences of internal modes of climate variability. One major question that needs to be answered related to precipitation extremes and characteristics is: How does the inter-annual, decadal, and multidecadal climate variability affect the occurrence of precipitation extremes relating to magnitude and frequency?

1.5.1 Extreme Precipitation Indices

Indices for precipitation extremes defined by the Expert Team on Climate Change Detection and Indices (ETCCDI) (WMO 2009) can be computed at each site to gain a clear understanding of changes in precipitation extremes during different phases. A total of 27 indices were developed by ETCCDI (WMO 2009) to describe particular characteristics of extremes, including frequency, amplitude, and persistence for temperature and precipitation. Nine extreme precipitation indices as defined by ETCCDI in Table 1.2 are explained in this section. The indices RX1day and RX5day refer to the maximum one-day and five-day precipitation in a given time period. The indices R10mm, R20mm, and Rnnmm are used to calculate the number of times a given value of threshold (viz., 10 mm, 20 mm, and “nn” mm) (WMO 2009) is exceeded. A threshold value of 25.4 mm is considered for “nn” in this study. Simple daily intensity index (SDII) and total precipitation in wet days (PRCPTOT) refer to average and total precipitation amounts of all wet days in a given time period, respectively. The time period used for the analysis can vary from a season to year. Consecutive dry days (CDD) and consecutive wet days (CWD) indices provide the largest number of consecutive dry and wet days in a given time period, respectively. Precipitation depth greater than or equal (less than) to 1 mm is used to categorize wet (dry) days in the calculation of SDII, PRCPTOT, CDD, and CWD indices. A few indices described in Table 1.3 require serially continuous (i.e., gap-free) precipitation datasets. Some of the indices can also be obtained from data with gaps (i.e., missing records), and they include RX1day, RX5day, CDD, and CWD. However, the indices may be underestimated due to the infilling process. Two recent studies (Goly and Teegavarapu 2014 and Teegaravapu et al. 2013) have documented the changes in several extreme precipitation indices in two phases of AMO and ENSO in the state of Florida, USA.

Table 1.3 Extreme precipitation indices and their explanation (WMO 2009)

Index	Description
RX1day	Maximum 1-day precipitation
RX5day	Maximum 5-day precipitation
SDII	Simple daily intensity index
R10mm	Count of precipitation days with DR greater than 10 mm
R20mm	Count of precipitation days with DR greater than 20 mm
Rnnmm	Count of days where DR greater than a threshold value
CDD	Consecutive dry days ($DR < 1$ mm)
CWD	Consecutive wet days ($DR \geq 1$ mm)
R95pTOT	Total precipitation due to wet days (>95th percentile)
R99pTOT	Total precipitation due to extremely wet days (>99 percentile)
PRCPTOT	Total precipitation in wet days ($DR > 1$ mm)
DR : Daily Rainfall	

1.5.2 Drought Characterization

1.5.2.1 Standard Precipitation Index (SPI)

Standard Precipitation Index (SPI) (WMO 2012), an internationally recognized index, developed by McKee et al. (1993, 1995), is useful to evaluate dry and wet conditions. It is generally used for drought monitoring; however, it is also very effective in analyzing wet periods. The only input for this conceptually simple index is the precipitation, requiring monthly data without gaps, with a minimum length of 20 to 30 years, but optimally a longer period, 50 or 60 years or more is recommended. The confidence level of the analysis and the length of the data are positively correlated. The length of water deficit or abundance due to drought and heavy precipitation can have different effects on soil moisture, streamflow, or groundwater supply on different timescales. SPI can be calculated for different intervals, to capture and analyze the effects, based on the point of interest. Standard Precipitation Index (SPI) calculation involves fitting a probability distribution (typically a gamma distribution) to 1-, 3-, 6-, and 12-month precipitation totals and then use of standard normal distribution to obtain SPI values. Probability density function of gamma distribution in standard form is given in Eq. (1.1). The variable α is the shape parameter. SPI values can be used to define dry and wet conditions as explained in Table 1.4.

$$f(x) = \frac{1}{\Gamma(\alpha)} x^{\alpha-1} e^{-x}, \quad x \geq 0 \quad (1.1)$$

An example of SPI calculation based on monthly precipitation observations at a rain gauge site (site name, Wakkanai and location; latitude, 45.4025000; longitude, 141.6686111) in Japan is provided in Fig. 1.2. A total of 78 years of monthly data is used for developing 3-month SPI. Teegavarapu (2016) has evaluated the changes in SPI for 155 sites in Japan and indicted more drought occurrences in ENSO warm phase (El Niño). Goly and Teegavarapu (2014) observed an opposite effect of ENSO in their study of drought occurrences in Florida.

Table 1.4 Identification of dry or wet conditions based on SPI

SPI Value	Dry or Wet Condition
2.0 and greater	Extremely wet
1.99 to 1.50	Very wet
1.49 to 1.00	Moderately wet
0.99 to -0.99	Near normal
-1.0 to -1.49	Moderately dry
-1.50 to -1.99	Severely dry
-2 and less	Extremely dry

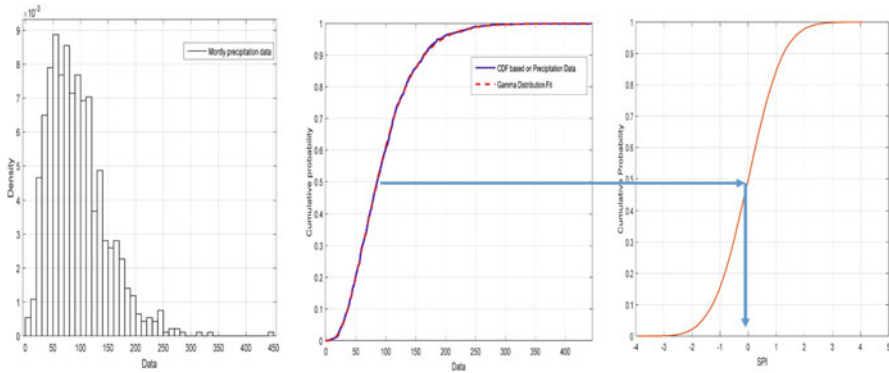


Fig. 1.2 Calculation of a 3-month SPI for a rain gauge site in Japan

1.6 Precipitation Characteristics

Changes in precipitation data characteristics based on available historical data can be evaluated for influences of oscillations using a number of indices. These indices are discussed in the following sections.

1.6.1 Inter-year and Intra-year Variations

Precipitation characteristics that vary within a year as well as over several years can be evaluated for influences of climate variability. Within year variations can be assessed at different temporal scales ranging from sub-hourly time intervals to seasons.

1.6.2 Storm Events Based on Inter-event Time Definition (IETD)

Rainfall time series can be considered as a series of rainfall pulses through time. Isolation of individual storm event from such a long record of p requires application of specific criteria to determine when an event begins and ends. One such criterion is inter-event time definition (IETD): Minimum temporal spacing without rainfall required to consider two rainfalls as belonging to different events, used for the statistical analysis of rainfall records. The concepts of IETD are illustrated in Figs. 1.3 and 1.4. If the period between pulses of rainfall is less than or equal to IETD, then the two pulses of rainfall are categorized as belonging to one event.

Fig. 1.3 Two storm events separated by a time interval

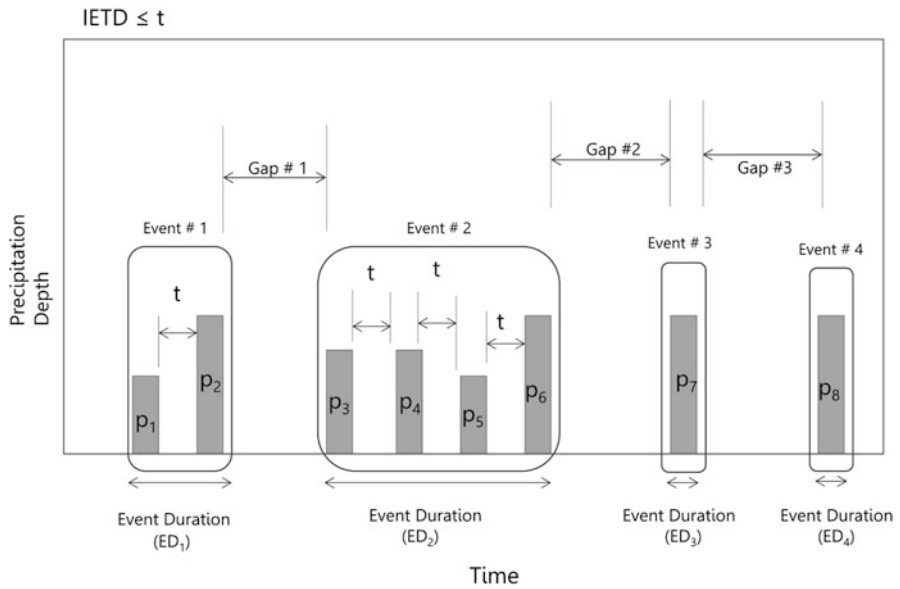
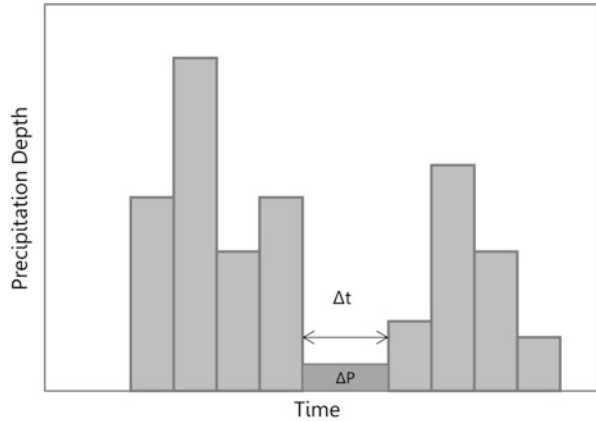


Fig. 1.4 Two storm events separated by a time interval

IETD can be equal to lag –time when autocorrelation is equal to zero. The inter-event time definition (IETD) is defined as the minimum temporal spacing without rainfall required to consider two rainfall events as belonging to different events (Adams and Papa 2000).

Two rainfall events are considered as distinct events if:

1. The precipitation (ΔP) that falls during a time interval between the events is less than a specific threshold value.
2. The time interval (Δt) is greater than a selected time interval (e.g., time of concentration).

The use of design storms based on IDF curves for stormwater management was evaluated by Adams and Howard (1986). The analytical probabilistic models for stormwater management models prescribed by Adams and Papa (2000) describe the need for identification of individual storms using inter-event time definition. Rainfall volumes, durations, intensities, and inter-event times can be characterized using exponential or gamma distributions (Behera et al. 2010) for use in analytical probabilistic models. The statistics of storm event characteristics are influenced by the values of IETD, and these can be analyzed in the context of climate variability and change. Pierce (2013) has documented changes in IETD of storms for AMO, PDO, and NAO in Florida, USA.

1.6.3 Wet and Dry Spells

Determining wet and dry spells can provide further information about the precipitation characteristics. Mean or total monthly rainfall values will give indication about how wet or dry the month was; however, determining the distribution of the rainfall can be essential when managing watersheds and flood or drought conditions. The conditions in the watershed will vary based on the distribution of the total rainfall over any interval. Precipitation threshold values can be established for evaluation of dry and wet thresholds; in general, a zero value of precipitation is ideal for consideration. Once the threshold is established, consecutive wet and dry days can be estimated as wet and dry spells, respectively. The length of each wet and dry spell can be used to calculate the mean length of wet and dry spell individually. The lengths of spells considering a threshold level are representative of regional rainfall patterns and can be evaluated for changes. The number of wet or dry spells that is equal or longer than a prefixed threshold value can be evaluated in different temporal windows that coincide with different phases of oscillations.

1.6.4 Transitions of Wet and Dry States

Transition probabilities associated with dry and wet spells are calculated based on conditions specified in Table 1.5. These probabilities are referred to as two-state first-order Markov chain probabilities.

Table 1.5 Rain or no-rain states in two consecutive time intervals for determination of transition probabilities

		Time interval ($i+1$)	
Time	$R_i > 0$	$R_{i+1} > 0$ [Wet–Wet]	$R_{i+1} = 0$ [Wet–Dry]
Interval (i)	$R_i = 0$	$R_{i+1} > 0$ [Dry–Wet]	$R_{i+1} = 0$ [Dry–Dry]

Two-state first-order Markov chain probabilities are given in Eqs. (1.2), (1.3), (1.4), and (1.5):

$$P_{11} = P_r (R_{i+1} > 0 \mid R_i > 0) \quad (1.2)$$

The variable P_{11} refers to probability of occurrence of positive precipitation in time interval $i + 1$ given the occurrence of positive precipitation in the previous interval, i :

$$P_{10} = P_r (R_{i+1} = 0 \mid R_i > 0) \quad (1.3)$$

The variable P_{10} refers to probability of no precipitation in time interval $i + 1$ given the occurrence of positive precipitation in the previous interval, i :

$$P_{01} = P_r (R_{i+1} > 0 \mid R_i = 0) \quad (1.4)$$

The variable P_{01} refers to probability of occurrence of precipitation in time interval $i + 1$ given no precipitation in the previous interval, i :

$$P_{00} = P_r (R_{i+1} = 0 \mid R_i = 0) \quad (1.5)$$

The variable P_{00} refers to probability of no precipitation in time interval $i + 1$ given no precipitation in the previous interval, i :

1.6.5 Persistence

Precipitation data can be assessed for serial autocorrelation using the time series at different temporal resolutions. The autocorrelation coefficient is also referred to as serial correlation coefficient. The first-order autocorrelation coefficient can be referred to as correlation coefficient of the first $N-1$ observations (observations), $\theta_1 \dots \theta_{N-1}$, and the next $N-1$ observations, $\theta_2 \dots \theta_N$. These two series are used for calculations of average values, and they are referred to as $\bar{\theta}_{(1)}$ and $\bar{\theta}_{(2)}$, respectively. The autocorrelation values can be obtained for different lag (t) values as given in Eq. (1.6):

$$\rho_t = \frac{\sum_{i=1}^{N-t} (\theta_i - \bar{\theta}_{(1)}) (\theta_{i+t} - \bar{\theta}_{(2)})}{\sqrt{\sum_{i=1}^{N-t} (\theta_i - \bar{\theta}_{(1)})^2} \sqrt{\sum_{i=2}^N (\theta_i - \bar{\theta}_{(2)})^2}} \quad (1.6)$$

For sufficiently large N , the autocorrelation at a specific lag can be defined by Eq. (1.7).

$$\rho_t = \frac{\sum_{i=1}^{N-t} (\theta_i - \bar{\theta}) (\theta_{i+t} - \bar{\theta})}{\sum_{i=1}^{N-t} (\theta_i - \bar{\theta})^2} \quad (1.7)$$

The variable $\bar{\theta}$ is the mean (average) of the entire available time series data. Autocorrelograms can be evaluated for two-sample datasets from two time periods that coincide with the temporal windows of the oscillation. Spatial variations in lag-1 autocorrelation values in Japan were noted in different phases of ENSO and PDO in a recent study reported by Teegavarapu (2016).

1.6.6 Seasonality

The seasonality index (SI) defined by Walsh and Lawler (1981) can be used to determine the intra-annual monthly distribution of precipitation. The SI can also be used for spatial representation of seasonal variability over regions, providing a better understanding of rainfall regimes. The SI, as given in Eq. (1.8), is the sum of the absolute deviations of the monthly rainfall from the mean monthly rainfall, divided by the total annual precipitation of the given year:

$$SI_i = \frac{1}{R_i} \sum_{n=1}^{n=12} \left| x_{i,n} - \frac{R_i}{12} \right| \quad (1.8)$$

where R_i is the total annual precipitation in a particular year and $x_{i,n}$ is the actual monthly rainfall in month n . The SI in Eq. (1.2) yields yearly indices, which can be qualified based on the established index values, to determine the degree of seasonality, shown in Table 1.6. Teegavarapu (2016) and Pierce (2013) evaluated seasonality index values for Japan and Florida, respectively, and concluded that warm and cool phases of PDO have strong influences on the spatial variability of seasonality of precipitation.

Table 1.6 Classification of seasonality index values and links to precipitation regimes (Walsh and Lawler 1981)

Seasonality index	Precipitation regime
<0.19	Precipitation spread throughout the year
0.20–0.39	Precipitation spread throughout the year, but with a definite wetter season
0.40–0.59	Rather seasonal with a short drier season
0.60–0.79	Seasonal
0.80–0.99	Marked seasonal with a long dry season
1.00–1.19	Most precipitation in <3 months
>1.20	Extreme seasonality, with almost all precipitation in 1–2 months

1.6.7 Changes to Extremes of Specific Duration and Frequency

Changes to extreme values of precipitation for different temporal durations in different phases of oscillations can be evaluated by developing depth–duration–frequency (DDF) or intensity-duration-frequency (IDF) curves. Data for two different temporal windows that coincide with the phases of oscillations can be used to fit probability distribution functions (PDFs) to characterize the precipitation extremes of different durations. Svensson and Jones (2010) in a recent survey of evaluation of rainfall frequency distributions have indicated that generalized extreme value (GEV) distribution is most frequently used to characterize rainfall extremes. Besides GEV, lognormal, three-parameter lognormal, and Pearson and log-Pearson distributions should also be evaluated for characterizing extreme precipitation data. Goodness-of-fit (GOF) hypothesis tests and performance measures such as mean absolute deviation (MAD) and mean square deviation (MSD) (Jain and Singh 1987) can be used to measure the relative goodness-of-fits of distributions to the data. GEV with a flexible three-parameter model expressed by a probability density function (PDF) given in Eq. (1.9) (Teegaravapu et al. 2013) is generally used to characterize precipitation extremes.

$$f(x) = \begin{cases} \frac{1}{\sigma} \exp\left(-\left(1 + k^o z_o\right)^{-\frac{1}{k^o}}\right) \left(1 + k^o z_o\right)^{-1 - \frac{1}{k^o}} & k^o \neq 0 \\ \frac{1}{\sigma} \exp\left(-z_o - \exp(-z_o)\right) & k^o = 0 \end{cases} \quad (1.9)$$

The variables k^o , σ , and μ refer to the shape, scale, and location parameters, respectively, and the value of $z_o = (x - \mu) / \sigma$. The parameters of the distribution can be estimated using maximum log-likelihood estimation (MLE) method or L-moment method. The maximum precipitation depth for each time interval is related with the corresponding return period from the cumulative distribution function (CDF). The maximum precipitation depth can be determined using a theoretical distribution function that is used to characterize the distribution of precipitation extremes.

1.6.7.1 Changing Intensity–Duration–Frequency Relationships

An example of DDF curves developed for four regions in the state of Florida, USA, in a recent study by Teegaravapu et al. (2013) using GEV is shown in Fig. 1.5. Precipitation extremes obtained from DDF curves developed for a specific return period indicate that the selection of temporal window coinciding with a specific phase of AMO is critical for hydrologic design. Regional differences in extreme precipitation depths based on DDF curves during different AMO phases are evident. Underestimation of design storms is possible when entire available historical data is used compared to the data obtained from one AMO phase alone.

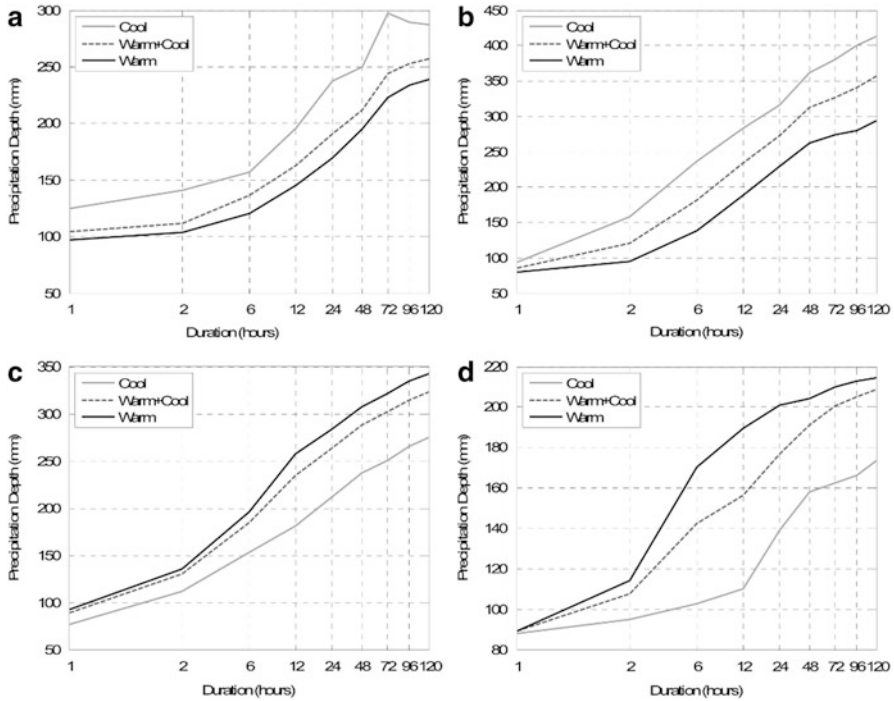


Fig. 1.5 Precipitation depth–duration–frequency curves for a 25-year return period during AMO warm, cool, and combined phases (cool and warm) for different stations: (a) North Florida, (b) Key West, (c) Palm Beach, and (d) Lake Okeechobee (Adopted from Teegaravapu et al. 2013)

1.6.8 Variations in Temporal Occurrences of Extremes

Changes in intra-year temporal occurrences of extremes caused due to climate variability of change have wide range of implications on water resources management. An example of such variations in occurrences is shown in Fig. 1.6 based on results from evaluation of precipitation extremes in two phases of AMO. Kernel density estimates (KDEs) using Gaussian kernels showing temporal occurrences of precipitation extremes for different durations are shown. It is evident from the figure that higher densities are seen in cool phase during earlier months of the year compared to those in warm phase. This suggests that flood realization potential is higher in earlier months of the year in the cool phase, and this requires adequate planning and preparation for any flood control management. In general, it has been noticed that precipitation extremes with higher magnitudes are occurring in AMO warm phase than in cool phase especially at durations higher than 24 h.

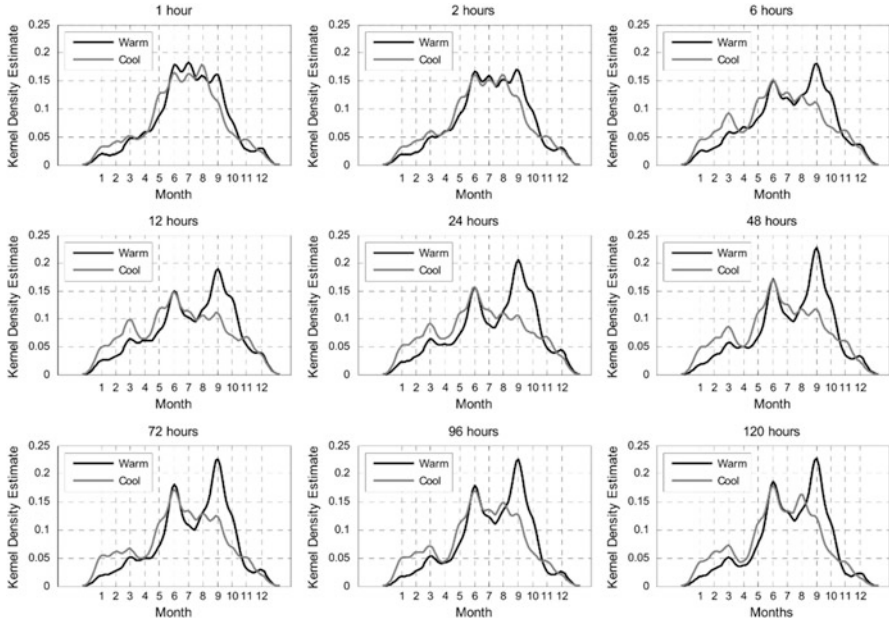


Fig. 1.6 Kernel density estimates of occurrences of precipitation extremes during AMO phases for nine temporal durations for cool (1970–1994) and warm (1942–1969) phases of AMO (Adapted from Teegavarapu et al. 2013)

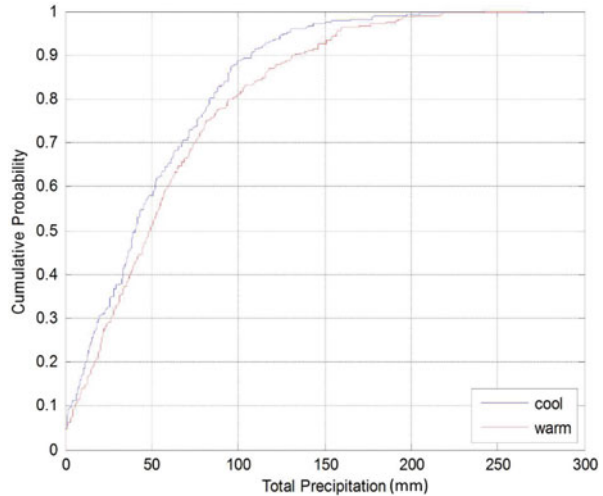
1.6.9 Temporal Distributions of In-Storm Precipitation

Temporal distribution defines the time distribution of rainfall amounts within a storm event. Synthetic rainfall distributions are commonly used for hydrologic design in many regions of the world. For example, the Soil Conservation Service (SCS) of the USA provides four types of curves referred to as types I, IA, II, and III that are applicable to different regions of the USA. The time distribution will provide information about early, central, and late peaking storms. Changes in temporal distribution of in-storm precipitation totals are noted for different storm events in Florida by Goly and Teegavarapu (2014). Late peaking storms are known to increase flood peaks and are of concern for disaster management agencies.

1.6.10 Antecedent Moisture Conditions (AMC)

Antecedent moisture conditions preceding extreme precipitation events of specific temporal duration can be evaluated for changes in two different phases of oscillations. Higher AMCs will lead to larger peak runoff volumes and discharges based on

Fig. 1.7 Non-exceedance probability curves for AMO cool and warm phases 5-day antecedent precipitation amounts (Adapted from Goly and Teegavarapu 2014)



extreme precipitation events, and these runoff discharges may sometimes exceed the design discharges that were used for hydrologic/hydraulic infrastructure. In a recent study, Goly and Teegavarapu (2014) have investigated the variations in AMC for multidecadal (e.g., AMO) and inter-year oscillations (e.g., ENSO). Figure 1.7 shows the non-exceedance plots of a 5-day antecedent precipitation amounts for AMO cool and warm phases. Higher exceedance probabilities can be noted for warm phase. Similar conditions of AMC for ENSO influences on precipitation patterns in Japan were noted in a recent study (Teegavarapu 2016). Hydrologic design discharges need to be reevaluated considering the influences of climate variability on extreme precipitation events.

1.7 Evaluations of Precipitation Variability Influenced by Teleconnections

1.7.1 Precipitation Data

Precipitation data at different temporal and spatial resolutions can be used for evaluation of influences of climate variability on extremes and characteristics. Serially continuous (data without gaps) and error-free and chronologically complete precipitation dataset is needed for evaluation of some of the indices discussed earlier in this chapter. Monthly data can be used for a handful of indices (i.e., seasonality, standard precipitation index). Daily data and data at finer temporal resolutions can be evaluated for short duration precipitation extremes and characteristics (Teegavarapu et al. 2013) including transition probabilities and autocorrelation.

1.7.2 Homogeneity Analysis and Tests

Precipitation data are initially evaluated for serial continuity, outliers, and homogeneity. Exploratory data analysis techniques (mostly graphical) can be used in the first step of preliminary assessment of data. Homogeneity evaluation can be carried out using Buishand's (Buishand 1982) or Alexandersson's standard normal homogeneity test (SNHT) (Alexandersson 1986) or von Neumann ratio test (Von Neumann 1941). Randomness of time series values can be tested with the help of runs test (Wald–Wolfowitz test) for use in statistical hypothesis tests.

1.7.3 Point Precipitation Data

Point-based precipitation data refers to observed data collected using a recording or a non-recording gauge. Gauge measurements are influenced by random and systematic errors and several others including gauge catch. In many instances extreme precipitation events are not recorded by gauges. Radar-based precipitation datasets can be used for assessments, with an acknowledgment of limitation that only comprehensive data from most recent decades are available. Infilling of precipitation datasets is required to obtain serially complete precipitation datasets in many situations. These datasets are critical for calculation and evaluation of a number of indices that are discussed earlier in this chapter. Some of those indices include autocorrelation, transition probabilities, IETD calculations, etc. A number of deterministic and stochastic interpolation methods that are available for estimation of missing precipitation data are documented by Teegavarapu and Chandramouli (2005). New methods based on improvised universal function approximation-based kriging (Teegavarapu 2007), association rule mining (Teegavarapu 2009), mathematical programming (Teegavarapu 2012), nearest neighbor, and clustering (Teegavarapu 2013) approaches are available for infilling missing data. Corrections to spatially interpolated data are recommended. These corrections may involve the use of single-best estimator methods (Teegavarapu 2009) or quantile-based methods (Teegavarapu 2014).

1.7.4 Gridded Precipitation Data

Gridded precipitation data based on spatially interpolated estimations from point observations from single-sensor (i.e., rain gauge) or multisensor estimates are widely available for spatial evaluation of precipitation. It is important to note that using such data may result in underestimation of higher-end extremes and overestimation of lower-end extremes. Goly and Teegavarapu (2014) indicate that both point and spatially complete gridded precipitation datasets are valuable for analysis.

Justifiable inferences about spatial variability in precipitation characteristics and extremes can be drawn when the two datasets are used independently. Goly and Teegavarapu (2014) indicated that variance deflation; over- and underestimation of lower- and higher-end extremes, respectively; and alteration of statistical distributions are inevitable consequences of spatial interpolation methods often used for generation of gridded datasets. In conclusion, inferences based on gridded precipitation data should be interpreted carefully.

1.7.5 Trend Evaluation

Trend analysis will help to (1) understand and confirm the existence (or nonexistence) of statistically significant changes in precipitation extremes or characteristics; (2) develop defensible (statistically) parametric and nonparametric methods for evaluation of changes in space and time; (3) develop and evaluate new methods or variants of existing trend evaluation methods considering issues related to homogeneity, data length, and others; and (4) ascertain and confirm any attributable reasons (natural climate variability influenced or anthropogenic changes) to the changes or trends. The number of sites selected for any study will depend on a number of factors: (a) long historical record length, (b) availability of error- and gap-free data records, and (c) availability of sites in watersheds with exhaustive hydrometeorological data. Smoothing methods and filters (e.g., moving average, LOWESS (derived from “locally weighted scatter plot smooth”) and Savitzky–Golay filter, and variants of LOWESS) can be used to assess the nonlinear variation of precipitation extremes with time. The following are the tasks that need to be completed for evaluation of trends:

1. Collect and evaluate the precipitation time series data at several sites in the region of interest for homogeneity issues.
2. Extract extremes and conduct analysis to check for existence of change points in the time series.
3. Develop and test nonparametric and parametric approaches for trend assessment considering issues such as serial autocorrelation, length of the data, temporal windows (moving and constant) and temporal windows linked to different phases of natural climate variability, or anthropogenic activity.
4. Assess natural or anthropogenic-based variations in extremes using detection and attribution methods.

Trend assessment can be carried out using nonparametric tests such as Spearman’s rho and Mann–Kendall tests. Modified Mann–Kendall test can be used if ranked data based on the sample indicates several ties. If strong serial autocorrelation exists at several lags that are higher than confidence limits as evaluated using autocorrelogram and by Ljung–Box Q-test (Ljung and Box 1978), trend-free pre-whitening can be employed. Serial autocorrelation affects the null distribution of trend tests, and therefore these tests and corrective procedures are required.

Change points in the precipitation time series can be identified using Pettitt's test (Pettitt 1979). Step change in mean or median values can be evaluated using several tests (e.g., distribution-free cumulative sum control chart (CUSUM) (nonparametric test), cumulative deviation (parametric), Worsley's likelihood ratio (parametric)). Parametric (e.g., two-sample t -test) and nonparametric (e.g., Rank Sum or Mann-Whitney) tests will also be used to evaluate statistically significant changes in mean and median values in two different data periods (two different temporal slices). A robust estimator of linear trend using Thiel-Sen trend line can be developed for each flow extreme time series. In case of parametric modeling, linear regression models can be developed and hypothesis tests can be used to evaluate the statistically significant slope parameter. Exhaustive evaluation of residuals needs to be carried out using Durbin-Watson test to check for autocorrelation in residuals, probability plots, and goodness-of-fit (GOF) hypothesis tests (e.g., Kolmogorov-Smirnov (KS) and Lilliefors test) for normality of residuals and autocorrelation function plots for visual assessment of serial autocorrelation at different lags. These tests can help in validating the assumptions of linear regression analysis. Spatial evaluation of trends can be carried out either by grouping the data into pooled datasets considering homogenous subregions defined by hydroclimatology and other physical features of the watersheds or basins in the region of interest or by using site-based trend assessment results. Methods for attribution and detection may be based on fingerprinting technique or its variants and time series analysis-based methods wherein noise is removed from the signal.

1.7.6 Biases Due to Missing and Filled Precipitation Data

Existence of missing data in precipitation time series will influence analysis of short- and long-term variations in precipitation based on different indices discussed in this chapter. Data filling may not always alter site-specific statistics of imputed data when spatial interpolation methods are used for temporal scales larger than a day (e.g., monthly, seasonal, or annual). However, data filling can lead to changes in probability distribution of data and significant biases when event-based analysis (such as daily or hourly extreme precipitation analysis) is performed. In some cases, spatial interpolation is only approach as temporal interpolation fails due to lack of high serial correlation at several lags in daily precipitation data. At temporal resolutions of a day or less, spatial interpolation alters probability distributions of data and changes the autocorrelation structure and dry and wet spell transitions (Teegavarapu 2014). Many research efforts have focused on analyzing the trends in precipitation data, but biases introduced in these trends due to data infilling techniques are rarely investigated. Therefore, evaluation of (1) bias in extreme precipitation data due to infilling of data gaps, (2) changes in long-term trends in extreme precipitation indices due to infilling, and (3) variations in probability distributions of infilled and unfilled datasets are essential. In a recent study, Teegavarapu et al. (2011) indicated

that infilling may lead to underestimation of both magnitude and frequency of heavy and very heavy precipitation events. Results show that infilling may also affect the spatial characteristics of extreme precipitation in the region. In general, it was noted that bias introduced by the data infilling increases as gaps (i.e., amounts of missing data) in precipitation data increase. Therefore, care should be taken while analyzing extreme precipitation events from precipitation data wherein gaps have been infilled or data with gaps is analyzed without infilling. Also, results from their study indicate that analysis of precipitation time series with missing data gaps infilled and unfilled data will lead to different conclusions about precipitation extremes and characteristics in different temporal windows of coupled oceanic–atmospheric oscillations.

1.8 Statistical Tests

Parametric and nonparametric statistical inference tests can be used to evaluate statistically significant differences in indices related to precipitation characteristics in two different phases of oscillations or two temporal windows.

1.8.1 *Parametric and Nonparametric Tests*

Samples for statistical hypothesis tests are generally identified based on datasets corresponding to different phases or temporal windows of oscillations. Parametric and nonparametric tests can be used to determine whether there is any statistically significant difference between the two population means or medians, respectively.

1.8.2 *Parametric Test: Two-Sample Unpaired T-Test*

A two-sample parametric t -test can be used to test null hypothesis that the two-sample datasets come from normal distributions with equal means but unknown variances. Satterthwaite's modified t -test (Satterthwaite 1946) is used when variances of two samples are unequal. Descriptions of two-sample parametric t -test and its modified version are provided in this section. Prior to the use of two-sample unpaired t -test, a two-sample F-test is used to evaluate the sample variances. The F-test evaluates the null hypothesis that the two-sample datasets come from normal distributions with the same variance. If the F-test confirms the null hypothesis, then the t -test statistic provided in Eq. (1.10) is calculated. The t -test statistic is calculated using Eqs. (1.10) and (1.11) when the sample variances based on two different sampling periods are equal:

$$t = \frac{|\bar{x}_1 - \bar{x}_2|}{\sqrt{\frac{n_1 + n_2}{n_1 n_2} \left(\frac{(n_1 - 1) S_1^2 + (n_2 - 1) S_2^2}{n_1 + n_2 - 2} \right)}} \quad (1.10)$$

The degrees of freedom (df) is defined by Eq. (1.11):

$$df = n_1 + n_2 - 2 \quad (1.11)$$

The variables n_1 and n_2 are the number of samples in dataset 1 and dataset 2, S_1^2 and S_2^2 are sample variances, and \bar{x}_1 and \bar{x}_2 are mean values of datasets 1 and 2, respectively. The unpaired two-sample t -test used for unequal sample variances is defined by Eqs. (1.12) and (1.13). The test is referred to as Satterthwaite's modified t -test (Satterthwaite 1946). The Welch–Satterthwaite modification Welch (1947) for degrees of freedom (df) in the case of this t -test is given in Eq. (1.13):

$$t = \frac{|\bar{x}_1 - \bar{x}_2|}{\sqrt{\frac{S_1^2}{n_1} + \frac{S_2^2}{n_2}}} \quad (1.12)$$

$$df = \frac{\left[\frac{S_1^2}{n_1} + \frac{S_2^2}{n_2} \right]^2}{\frac{S_1^4}{n_1^2 (n_1 - 1)} + \frac{S_2^4}{n_2^2 (n_2 - 1)}} \quad (1.13)$$

Application of parametric two-sample t -test requires normality of the samples as requisite condition. Sample data individually from two datasets or groups can be tested for normality. Normality can be confirmed using visual checks using normal probability plots (Mage 1982; McBean and Rovers 1998) initially. After initial confirmation of normality, several statistical hypothesis tests such as Kolmogorov–Smirnov (Smirnov 1939; Sheskin 2003), Lilliefors (1967), Jarque–Bera (1987), and chi-Square goodness-of-fit (Corder and Foreman 2009) tests can be used for additional confirmations. A well-known Lilliefors test as a two-sided goodness-of-fit test for normality is applicable for situations where a fully specified null distribution is not known. In case of the Kolmogorov–Smirnov (KS) test, the null distribution of the sample needs to be completely specified. Alternatively, Jarque–Bera test can help check the validity of null hypothesis that the data comes from a normal distribution with an unknown mean and variance, and chi-square test can be used to evaluate the null hypothesis that the data follows a normal distribution using parameters (mean and variance) estimated from the sample. It is important to note that chi-square test is sensitive to the number of bins used for grouping the sample data. If datasets do not conform to normality, logarithmic, square, square root, and several other transformations recommended by Helsel and Hirsch (2002) are initially evaluated. If none of these transformations are helpful to achieve normality,

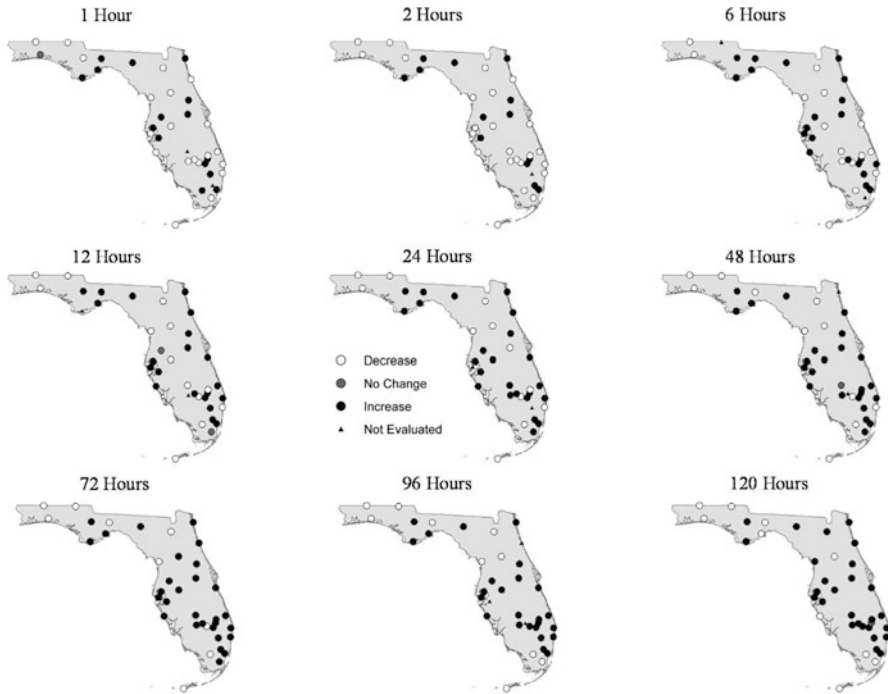


Fig. 1.8 Statistically significant changes in the extreme precipitation depths during two AMO phases for nine different durations (Adapted from Teegaravapu et al. 2013, Journal of Hydrology)

then a power transform such as Box–Cox (Box and Cox 1964) transformation can be used. The parameter of such power transform is obtained by optimization of a log-likelihood function with an objective of maximization of log-likelihood function. If all transformations fail, nonparametric tests can be adopted. Results for statistically significant changes in extreme precipitation depths (Teegaravapu et al. 2013) during two phases of AMO using two-sample unpaired t -test are shown in Fig. 1.8.

1.8.3 Nonparametric Test: Mann–Whitney U -Test

The Mann–Whitney U -test can be used to evaluate the null hypothesis (H_0) that data from two samples are from continuous distributions with equal medians, against the alternative (H_a) that they are not. The test assumes that the two samples are independent. The samples can be of different lengths. In order to apply the Mann–Whitney U -test, the precipitation datasets for two samples (e.g., data from El Niño and La Niña phases or two phases of any oscillation) can be used. The variables n_1 and n_2 are used to refer to the number elements in each sample. The data in each sample l , n_l are then ranked from lowest to highest, including tied rank values where

appropriate. The equations related to Mann–Whitney U -test statistic are as follows as defined by Corder and Foreman (2009):

$$U_l = n_1 n_2 + \frac{n_i (n_i + 1)}{2} - \sum R_l \quad (1.14)$$

$$\bar{x}_u = \frac{n_1 n_2}{2} \quad (1.15)$$

$$S_u = n_1 n_2 + \sqrt{\frac{n_1 n_2 (n_1 + n_2 + 1)}{12}} \quad (1.16)$$

$$Z^* = \frac{U_l - \bar{x}_u}{S_u} \quad (1.17)$$

The variable S_u is the standard deviation and R_l is the rank from the sample l of interest and \bar{x}_u is the mean. The variable Z^* is the z -score for a normal approximation of the data. The null hypothesis is rejected if the calculated Z^* statistic is greater than the selected critical value at 5 % significance level (α) obtained from the standard normal distribution table. The notation used in Eqs. (1.14), (1.15), (1.16), and (1.17) in this section is borrowed from Teegavarapu et al. (2013).

1.8.4 Bootstrap Sampling and Confidence Intervals

The use of bootstrap sampling methods (Efron 1979; Efron and Gong 1983) and finally the generation of confidence intervals can help make inferences about the sample statistics when limited numbers of datasets related to precipitation extremes or indices exist due to missing data or other reasons. Bootstrap sampling method (Efron and Tibshirani 1993) can be used to obtain samples from data in each phase of the oscillation or a specific temporal window, and confidence intervals on sample mean statistic can be developed. A general procedure of bootstrap sampling methodology explained by Davison and Hinkley (1997) and Teegavarapu et al. (2013) is adopted in this section. The notation used for explaining the bootstrap confidence interval generation is also based on Davison and Hinkley (1997). The sample values y_1, y_2, \dots, y_n are thought of as the outcomes of independent and identically distributed (iid) random variables Y_1, Y_2, \dots, Y_n whose cumulative distribution function (CDF) is denoted by F . The estimate of F denoted by \hat{F} is obtained using data y_1, y_2, \dots, y_n . The following steps are carried out (Davison and Hinkley 1997) to obtain bootstrap sampling confidence intervals:

- Bootstrap (re) sample $y_1^*, y_2^*, \dots, y_n^*$ $iid \hat{F}$ are obtained from the original samples allowing repetitions.

- \widehat{F} , an estimator of F , is obtained nonparametrically using empirical distribution function (EDF) of the original data, i.e., by placing a probability of “ $1/n$ ” at each data value from sample y_1, y_2, \dots, y_n .
- Sample mean statistic $\widehat{\theta}^*$ is computed from bootstrap sample $y_1^*, y_2^*, \dots, y_n^*$.
- The above steps are repeated “ N ” times, to obtain N sample means $\widehat{\theta}_1^*, \widehat{\theta}_2^*, \dots, \widehat{\theta}_N^*$. The practical size of “ N ” depends on the tests to be run on the data.

The size of “ N ” recommended by Chernick (2007) is 1,000 and 10,000 for evaluating the sample statistic and confidence intervals, respectively. In the current study, these values are used. After N samples are obtained, normally approximated confidence intervals are computed for the uncertainty assessment. If $\widehat{\theta}$ (estimated mean of original data) is approximately normal, then $\widehat{\theta} \sim N(\theta + \beta, v)$. The confidence interval (CI) of θ for known bias ($\beta = \beta(F)$) and variance ($v = v(F)$) (Davison and Hinkley 1997) is given in:

$$CI = \widehat{\theta} - \beta \pm Z_\alpha \cdot v^{1/2} \tag{1.18}$$

$$\text{where, } \beta(F) \doteq \beta(\widehat{F}) \doteq b = \overline{\widehat{\theta}^*} - \widehat{\theta}, \tag{1.19}$$

$$v(F) \doteq v(\widehat{F}) \doteq v = \frac{1}{N-1} \sum_{i=1}^N (\widehat{\theta}_i^* - \overline{\widehat{\theta}^*})^2 \tag{1.20}$$

at 95 % confidence interval, $\alpha = 0.025$, $Z_\alpha = -1.96$

The variable $\overline{\widehat{\theta}^*}$ is the mean of $\widehat{\theta}_1^*, \widehat{\theta}_2^*, \dots, \widehat{\theta}_N^*$ and Z_α is the α quantile of the standard normal distribution.

In a recent study, uncertainty assessment of mean precipitation extremes is performed by Teegaravapu et al. (2013) using bootstrap sampling methodology. The 95 % confidence intervals using bootstrap resampling with normal approximation are computed using a total of 10,000 bootstrap samples that are obtained from data for each phase. The flowchart shown in Fig. 1.9 provides the steps required to estimate confidence intervals. These intervals can be computed at different spatial scales (individual rain gauges, different homogeneous rainfall areas and regions). Teegaravapu et al. (2013) report that in general considering the lower limit, the higher values of extremes are observed in AMO warm phase than in the cool phase for all durations, and for the upper limit, higher precipitation extremes are realized in AMO cool phase compared to those in AMO warm phase up to a 12-h duration. However, for durations equal or above 24 h, precipitation extremes are higher in warm phase compared to those in cool phase.

1.9 Wavelet-Based Methods and Analysis

Wavelet analysis can be used to evaluate the temporal patterns of oscillations and precipitation (Goly and Teegavarapu 2014). Continuous wavelet transform (CWT) allows the study of the temporal structure of precipitation and makes inferences on the influence of oscillation patterns. An example of the continuous wavelet transform power spectrum plots of total precipitation during dry season for continental and peninsular regions of Florida, USA, adopted from a recent study by Goly and Teegavarapu (2014) is shown in Fig. 1.9. The spectrum plots can be compared to those of AMO and ENSO oscillations mean index during dry season. A common time span of 1915–2011 is used for generation of the plots for

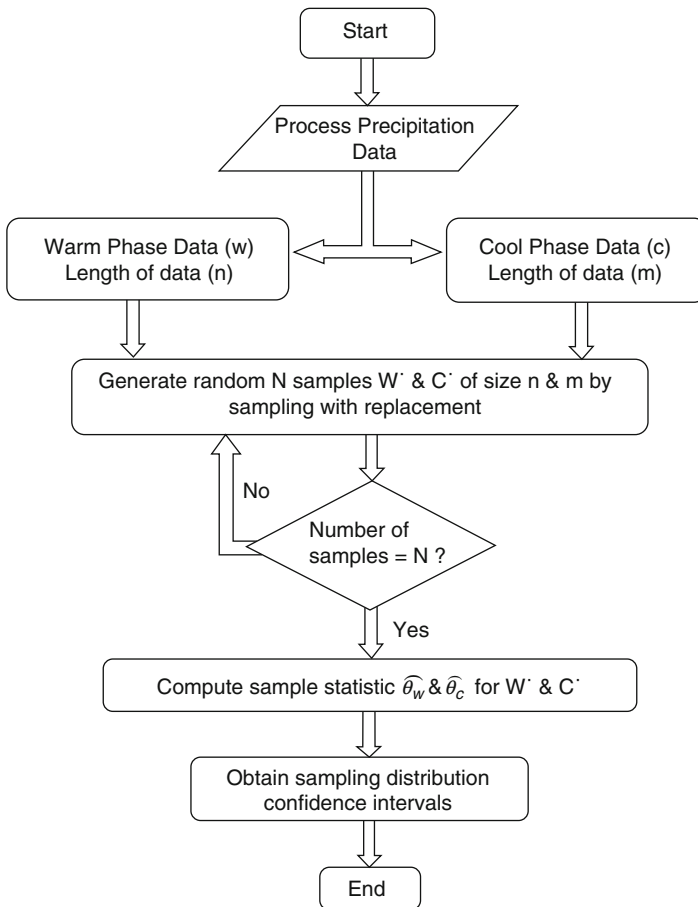


Fig. 1.9 Bootstrap sampling approach for the determination of confidence intervals (Adapted from Teegaravapu et al. 2013)

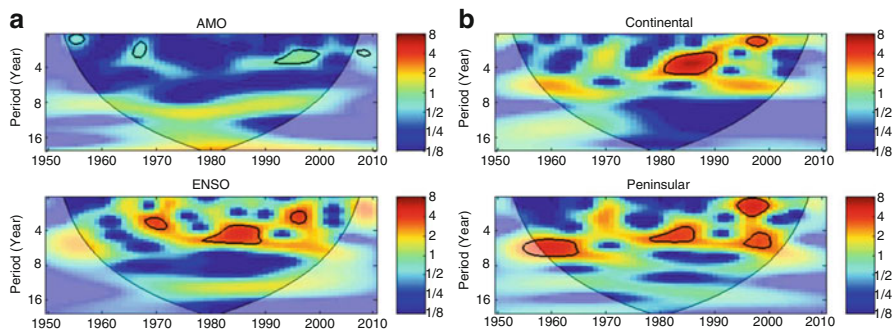


Fig. 1.10 Continuous wavelet power spectrum of (a) oceanic–atmospheric oscillation climate indices (dry season) and (b) precipitation (dry season) for continental and peninsular regions of Florida. The *thick black* contours designate the 5% significance level against red noise (Adapted with permission from Goly and Teegavarapu 2014)

both the oscillation indices. The statistical significance of the peaks in the wavelet spectrum was tested using Monte Carlo methods against a lag-1 autoregressive red noise background. The peaks with greater than 95% confidence interval are shown by thick black contours. AMO with a cycle of approximately 70 years is clearly apparent in this wavelet power spectrum plot shown in Figure 1.10. Similar plot for ENSO shows a much smaller wavelength with a recurrence period of 2–7 years. Significant power in this band was observed during 1940–1960, 1965–1972, 1978–1990, and 1996–1999 years in the wavelet spectrum of ENSO. A look at each power spectrum plot will suggest that in both continental and peninsular regions of state of Florida, significant power at the 5% significance level is evidenced and coincident with the patterns exhibited by ENSO is noted.

1.10 Regional Hydroclimatology Influences

In many regions around the world, local hydroclimatology may play a major role in restricting spatial and temporal influences of oscillations. Temporal shift in the occurrences of extremes from cool to warm phases or vice versa and distribution of intra-annual extremes will have impact on operation of hydrologic and hydraulic structures. Synthetic design storms generally used for hydrologic design and DDF curves need to be revisited and revised considering the occurrences and magnitudes of precipitation extremes in different phases of oscillations.

1.11 Influences of Individual and Coupled Oscillations

Two or multiple teleconnections influencing regional hydrology simultaneously in specific temporal windows may increase or decrease the frequency and magnitudes of extreme precipitation events and influence intra-annual temporal occurrences of extremes. Teegaravapu et al. (2013) suggest that emphasis should be placed on those temporal windows in which the combined influences of two or more teleconnections lead to rare extremes and data selection for design should be representative of these extremes. Site-specific extremes for hydrologic design confined to one specific region are routinely carried out. However, consideration of region-specific influences of climate variability at different spatial and temporal scales is recommended. Goly and Teegavarapu (2014) in a recent work documented an exhaustive study of combined influences of AMO and ENSO on precipitation extremes and characteristics in the state of Florida, USA. They conclude that precipitation extremes and characteristics are influenced by the two-coupled oceanic-atmospheric phenomena, with seasonally and spatially varying signatures in Florida. Essential climatic variables in many regions across the world are influenced more than one oscillation. A few examples of such multiple influences in different regions of the world include PDO and ENSO in Japan; ENSO, IOD, and MJO in India; and PDO, AMO, ENSO, and NAO in the USA. When multiple oscillations influence the precipitation regimes in a particular region, it is often difficult to evaluate combined influences or associate a particular pattern or change in precipitation to one specific oscillation. This is mainly due to lack of long-term precipitation data and the varying and overlapping temporal windows of intra-year, decadal, and quasi-decadal and multidecadal oscillations.

1.12 Influences of Oscillations on Precipitation: Spatial Extent

Regional and global influences of oscillations on precipitation and temperature extremes are documented in several studies (e.g., Teegavarapu 2013). However, in any given region, the spatial extent of any oscillation is not clearly delineated due to lack of dense observational network of rain gauges or reliable gridded data at a spatial resolution that is adequate to define the spatial extent of the influences. In recent studies availability of gridded precipitation data has helped in specifying spatial extents of influences. Teegaravapu et al. (2013) and Goly and Teegavarapu (2014) documented spatially uniform and nonuniform influences of ENSO and AMO in the state of Florida, USA, respectively, using gridded precipitation data. In the case of AMO, differences in the nature of influences especially in spatial extents in two phases were noted due to thermic and hyperthermic (in continental and peninsular regions) soil regimes in the state of Florida. In few regions of the world (e.g., the southeastern USA, Japan, and India), the paths of hurricane or

cyclone landfalls will influence the spatial variability of precipitation extremes. In the southern part of Florida, USA, precipitation extremes of longer durations are limited to regions that frequently experience hurricane landfalls.

1.13 Meteorologically Homogenous Areas

Evaluation of climate variability influences can be evaluated for regions that are classified as meteorologically homogeneous areas. These areas are developed by hydrologists and meteorologists based on information about the regional variations of precipitation, temperature, and other hydroclimatic variables. Teegaravapu et al. (2013) have used meteorologically homogeneous areas developed by a local water management agency in South Florida for evaluation of influences of AMO on precipitation extremes and characteristics. They found that there are differences in how AMO influences precipitation extremes in different areas. In many instances, Köppen–Geiger climate classification (Kottek et al. 2006) for a specific region can be beneficial in delineating the region into several homogenous climate zones.

1.14 Relating Indices and Precipitation Depths

Relationship between monthly oscillation indices of AMO, ENSO, PDO, and others and precipitation depths can be established and evaluated. A simple correlation-based analysis using monthly precipitation totals and lagged values of indices can reveal useful relationships that can help in forecasting seasonal precipitation totals. Spatially and temporally variable SST anomalies and variations in other climatic variables in different regions of the world can be used to establish the links.

1.15 Forecasts Based on Oscillations

Information about the hydroclimatic variables and their links to coupled oceanic–atmospheric oscillations can be beneficial to water management agencies involved in the planning for future water uses. Strong relationships between rainfall occurrences and streamflows have been observed in several parts of the world with variables that relate to the manifestation of teleconnections. Strong correlations between sea surface temperatures (SSTs) and streamflows (Dawod and El-Rafy 2002; Beek 2010) are examples of such relationships. Dawod and El-Rafy also report the links between the annual River Nile flows and SSTs at different locations in Indian Ocean and Pacific Ocean. An example of predictability of the flow is in the next hydrologic year (Beek 2010) using information available at the end of June. A high correlation between predicted set of flows and observed flows suggests

the utility of multiple linear regression equation linking flow and SSTs. Seasonal forecasts using climate change information are linked to analogue years through the use of historical climate records (Ludwig 2009). ENSO is strongly correlated with one or more hydroclimatic variables in several regions around the globe. These strong correlations can be used for seasonal rainfall and streamflow forecasts. Souza and Lall (2003) report the utility of using NINO3.4 (an indicator used to define the ENSO state) and North Atlantic Dipole index to forecast streamflows in northeast Brazil. Australian rainfall amounts were linked to El Niño by Chiew et al. (1998) and Southern Oscillation (SO) index (Chiew et al. 2003). Similar links in general will help in futuristic seasonal to yearly forecasts of rainfall helping water resources management professionals. In general teleconnections can be used for seasonal climate forecasts with benefits to water resources management. Water allocation can be improved if seasonal forecasts are available (Stone et al. 1996), and similarly future rainfall forecasts can be extremely beneficial to agrarian communities especially in arid and semiarid regions. Seasonal forecasts may help in water pricing and also developing plans for water use restrictions (Ludwig 2009).

1.16 Conclusions

Evaluation of influences of individual and coupled inter-year, decadal and multi-decadal, coupled oceanic–atmospheric oscillations on precipitation characteristics and extremes is the focus of this chapter. Precipitation regime changes are known to be influenced by several coupled oceanic–atmospheric oscillations around the globe. Exhaustive evaluation of individual and combined influences of these oscillations, descriptive extreme index-based assessment of precipitation extremes and changes in rainfall characteristics, identification of spatially varying influences of oscillations on dry and wet spell transition states, antecedent precipitation prior to extreme events, intra-event temporal distribution of precipitation, and changes in temporal occurrences of extremes is discussed in this chapter. Understanding these oscillations and their influences focusing on different spatial scales and temporal resolutions considering multiple duration-specific precipitation extremes is critical for flood control, water supply management, and hydrologic design. Parametric and nonparametric statistical tests using long-term precipitation data at point and grid scale can be used to assess statistically significant changes in the precipitation characteristics from one phase to another of each oscillation. Understanding of influences of oscillations on precipitation variability with regional hydroclimatology defining the spatial extent of these influences is critical for hydrologic analysis, design, and flood control management. This chapter presented an overview of oscillations and their possible influences on precipitation characteristics and extremes. Wherever possible, results from precipitation data analysis from regions influenced by single and multiple oscillations are used to explain the nature of variability in precipitation extremes and characteristics.

Acknowledgments The author would like to acknowledge the assistance provided by Ms. Milla Pierce in the preparation of this chapter.

References

- Adams BJ, Howard CDD (1986) Pathology of design storms. *Canad Water Resour J* 11(3):49–55
- Adams BJ, Papa F (2000) Urban stormwater management planning with analytical probabilistic models. Wiley, New York
- Alexandersson HA (1986) Homogeneity test applied to precipitation data. *J Climatol* 6(6):661–675
- Beek EV (2010) Managing water under current climate variability. In: Ludwig F, Kabat P, Schaik H, Valk M (eds) *Climate change adaptation in water sector*. Earthscan, London
- Behera P, Guo Y, Teegavarapu RSV, Branham T (2010) Evaluation of antecedent storm event characteristics for different climatic regions based on inter-event time definition (IETD). In: *Proceedings of the world environmental and water resources congress 2010, ASCE Conference Proceedings*. doi:[10.1061/41114\(371\)251](https://doi.org/10.1061/41114(371)251)
- Box GEP, Cox DR (1964) An analysis of transformations. *J R Stat Soc* 26(2):211–252
- Buishand TA (1982) Some methods for testing the homogeneity of rainfall records. *J Hydrol* 58(1–2):11–27
- Chernick MR (2007) *Bootstrap methods: a guide for practitioners and researchers*. Wiley-Interscience, Hoboken
- Chiew FHA, Piechota TC, Dracup JA, McMahon TA (1998) El Niño southern oscillation and Australian rainfall, streamflow and drought: links and potential for forecasting. *J Hydrol* 204:138–149
- Chiew FHS, Zhaou SL, McMahon TA (2003) Use of seasonal streamflow forecasts in water resources management. *J Hydrol* 270:135–144
- Corder WG, Foreman DI (2009) *Nonparametric statistics for non-statisticians*. Wiley, Hoboken
- Cronin TM (2009) *Paleoclimates: understanding climate change past and present*. Columbia University Press, New York
- Dai A, Fung J, Del Genio A (1997) Surface observed global land precipitation variations during 1900–1988. *J Clim* 11:2943–2962
- Davison AC, Hinkley DV (1997) *Bootstrap methods and their applications*
- Dawod MAA, El-Rafy MA (2002) Towards long range forecast of Nile Flood, *Proceedings of the fourth conference on meteorology and sustainable development*. Meteorologist Specialist Association, Cairo
- Efron B (1979) Bootstrap methods: another look at the jackknife. *Ann Stat* 7:1–26
- Efron B, Gong G (1983) A leisurely look at the bootstrap, the jackknife, and cross validation. *Am Stat* 37:36–48
- Efron B, Tibshirani R (1993) *An introduction to the bootstrap*. Chapman and Hall, London
- Enfield DB, Mestas-Nunez AM, Trimble PJ (2001) The Atlantic multidecadal oscillation and its relation to rainfall and river flows in the continental U.S. *Geophys Res Lett* 28(10):2077–2080
- Ghil M (2002) Natural climate variability. In: MacCraken MC, Perry JS (eds) *Encyclopedia of global environmental change—Volume 1, The earth system—physical and chemical dimensions of global environmental change*. Wiley, Chichester, pp 544–549
- Goly A, Teegavarapu RSV (2012) Influence of teleconnections on spatial and temporal variability of extreme precipitation events in Florida. *World Environ Water Resour Congress 2012*:1899–1908. doi:[10.1061/9780784412312.190](https://doi.org/10.1061/9780784412312.190)
- Goly A, Teegavarapu RSV (2014) Individual and coupled influences of AMO and ENSO on regional precipitation characteristics and extremes. *Water Resour Res* 50. doi:[10.1002/2013WR014540](https://doi.org/10.1002/2013WR014540)
- Gurdak JJ, Hanson RT, Green TR (2009) Effects of climate variability and change on groundwater resources of the United States, Fact Sheet 2009–3074., United States Geological Survey

- Helsel DR, Hirsch RM (2002) Statistical methods in water resources, Book 4, hydrologic analysis and interpretation, United States Geological Survey
- Hurrell JW, Van Loon H (1995) Decadal Variations in Climate Associated with the North Atlantic Oscillation. National Center for Atmospheric Research, Boulder
- Jain D, Singh VP (1987) Comparison of some flood frequency distributions using empirical data. In: Singh VP (ed) Hydrologic frequency modeling. Reidel, Dordrecht, pp 467–485
- Jarque CM, Bera AK (1987) A test for normality of observations and regression residuals. *Int Stat Rev* 55(2):163–172
- Koch-Rose M, Berry L, Bloetscher F, Hernández Hammer N, Mitsova-Boneva D, Restrepo J, Root T, Teegavarapu R (2011) Florida water management and adaptation in the face of climate change. Florida Climate Change Task Force
- Kottek M, Grieser J, Beck C, Rudolf B, Rubel F (2006) World map of Köppen-Geiger climate classification updated. *Meteorol Z* 15(3):259–263
- Lilliefors HW (1967) On the Kolmogorov-Smirnov test for normality with mean and variance unknown. *J Am Stat Assoc* 62(318):399–402
- Ljung G, Box G (1978) On a measure of lack of fit in time series models. *Biometrika* 65:297–303
- Ludwig F (2009) Using seasonal climate forecasts for water management. In: Ludwig F, Kabat P, Schaik HV, Van Der Valk M (eds) Climate change adaptation in the water sector. Earthscan Publishers, London
- Mage DT (1982) An objective graphical method for testing normal distributional assumptions using probability plots. *Am Stat* 36(2):116–120
- Mantua NJ, Hare SR, Zhang Y, Wallace J, Francis R (1997) A Pacific interdecadal oscillation with impacts on salmon production. *Bull Am Meteorol Soc* 78:1069–1079
- Mantua NJ, Hare SR (2002) The Pacific decadal oscillation. *J Oceanogr* 58(1):35–44
- McBean AE, Rovers FA (1998) Statistical procedures for analysis of environmental monitoring data and risk assessment. Prentice Hall, Upper Saddle River
- McKee TB, Doesken NJ, Kleist J (1995) Drought monitoring with multiple timescales. In: Proceedings of the ninth conference on applied climatology, Dallas, TX, 15–20 January 1995. Boston American Meteorological Society, pp 233–236
- McKee TB, Doesken NJ, Kleist J (1993) The relationship of drought frequency and duration to time scale. In: Proceedings of the eighth conference on applied climatology, Anaheim, California, 17–22 January 1993. American Meteorological Society, Boston, pp 179–184
- Newman M, Compo G, Alexander M (2003) ENSO-forced variability of the Pacific decadal oscillation. NOAA-CIRES Climate Diagnostic Center, Boulder. NOAA. 013
- Pettitt AN (1979) A non-parametric approach to the change-point problem. *Appl Stat* 28(2): 126–135
- Pierce M (2013) Influences of decadal and multidecadal oscillations on regional precipitation extremes and characteristics, Thesis, Florida Atlantic University
- Rosenzweig C, Hillel D (2008) Climate variability and the global harvest: impacts of El Nino and other oscillations on agroecosystems. Oxford University Press, New York
- Satterthwaite FE (1946) An approximate distribution of estimates of variance components. *Biom Bull* 2:110–114
- Schneider N, Cornuelle B (2005) The forcing of the Pacific decadal oscillation. *J Clim* 18(2005):4255–4273
- Sheskin DJ (2003) Handbook of parametric and nonparametric statistical procedures. Chapman and Hall/CRC, Boca Raton, FL
- Smirnov NV (1939) On the estimation of the discrepancy between empirical curves of distribution for two independent samples. (Russian). *Bull Moscow Univ* 2:3–16
- Souza FA, Lall U (2003) Seasonal to interannual ensemble streamflow forecasts for Ceara, Brazil: application of a multivariate, semiparametric algorithm. *Water Resour Res* 39
- Stone RC, Hammer GL, Marcussen T (1996) Prediction of global rainfall probabilities using phases of the Southern Oscillation Index. *Nature* 384:252–255
- Svensson C, Jones D (2010) Review of rainfall frequency estimation methods. *J Flood Risk Manag* 3:296–313

- Teegaravapu RSV, Goly A, Obeysekera J (2013) Influences of Atlantic multidecadal oscillation phases on spatial and temporal variability of regional precipitation extremes. *J Hydrol* 495: 74–93
- Teegaravapu RSV (2009) Estimation of missing precipitation records integrating surface interpolation techniques and spatio-temporal association rules. *J Hydroinf* 11(2):133–146
- Teegaravapu RSV (2010) Modeling climate change uncertainties in water resources management models. *Environ Model Softw* 25(10):1261–1265
- Teegaravapu RSV (2012) Spatial interpolation using non-linear mathematical programming models for estimation of missing precipitation records. *Hydrol Sci J* 57(3):383–406
- Teegaravapu RSV (2007) Use of universal function approximation in variance-dependent interpolation technique: an application in Hydrology. *J Hydrol* 332:16–29
- Teegaravapu RSV (2013) *Floods in a changing climate: extreme precipitation*. Cambridge University Press, Cambridge, UK
- Teegaravapu RSV (2014) Statistical corrections of spatially interpolated missing precipitation data estimates. *Hydrol Process* 28(11):3789–3808
- Teegaravapu RSV (2016) Evaluation of trends and variability in monthly sea level, temperature and precipitation of Japan: links to climate variability and change. Technical Report, Research Center for Urban Safety and Security (RCUSS). Kobe University, Kobe
- Teegaravapu RSV, Chandramouli V (2005) Improved weighting methods, deterministic and stochastic data-driven models for estimation of missing precipitation records. *J Hydrol* 312:191–206
- Teegaravapu RSV, Nayak A, Pathak C (2011) Assessment of long-term trends in extreme precipitation: implications of in-filled historical data and temporal window-based analysis. In: Proceedings of the 2011 world environmental and water resources congress, doi:[10.1061/41173\(414\)419](https://doi.org/10.1061/41173(414)419)
- USGS (2011) Evidence of multidecadal climate variability in the Gulf of Mexico. USGS
- Von Neumann J (1941) Distribution of the ratio of the mean square successive difference to the variance. *Ann Math Stat* 12:367–395
- Wallace JM, Gutzler DS (1980). Teleconnections in the geopotential height field during the northern hemisphere winter. Department of Atmospheric Sciences, University of Washington, *Monthly Weather Review*
- Walsh PD, Lawler DM (1981) Rainfall seasonality: description, spatial patterns and change through time. *Weather* 36:201–208
- Welch BL (1947) The generalization of student's problem when several different population variances are involved. *Biometrika* 34(1–2):28–35
- WMO (2009) Guidelines on analysis of extremes in a changing climate in support of informed decisions for adaptation. WMO, Geneva
- WMO (2012) Standard precipitation index user guide, World Meteorological Organization (WMO), WMO-No: 1090. WMO, Geneva
- Zhang Y, Wallace J, Battisti D (1996) ENSO-like interdecadal variability: 1900–93. Department of Atmospheric Sciences, University of Washington, Seattle, Washington